

Non-perturbative renormalization of four-quark operators and B_K with Schrödinger functional scheme in quenched domain-wall QCD

Y. Nakamura^{*a†} and Y. Taniguchi^{a,b} for CP-PACS Collaboration

^aGraduate School of Pure and Applied Sciences, University of Tsukuba, Tsukuba, Ibaraki 305-8571

^bCenter for Computational Sciences, University of Tsukuba, Tsukuba, Ibaraki 305-8577

We present non-perturbative renormalization factors for $\Delta S = 2$ four-quark operators in quenched domain-wall QCD using the Schrödinger functional method. Non-perturbative renormalization factor for B_K is evaluated at hadronic scale. Combined with the non-perturbative RG running obtained by the Alpha collaboration, our result yields renormalization factor which converts lattice bare B_K to the renormalization group invariant one. We apply the renormalization factor to bare B_K previously obtained by the CP-PACS collaboration with the quenched domain-wall QCD(DWQCD). We compare our result with previous ones obtained by perturbative renormalization factors, different renormalization schemes or different quark actions. We also show that chiral symmetry breaking effects in the renormalization factor are numerically small.

*The XXV International Symposium on Lattice Field Theory
July 30 - August 4 2007
Regensburg, Germany*

*Speaker.

†E-mail: nakayou@het.ph.tsukuba.ac.jp

1. Introduction

The Kaon B parameter

$$B_K = \frac{\langle \bar{K}^0 | \bar{s} \gamma_\mu (1 - \gamma_5) d \cdot \bar{s} \gamma_\mu (1 - \gamma_5) d | K^0 \rangle}{(8/3) \langle \bar{K}^0 | \bar{s} \gamma_\mu \gamma_5 d | 0 \rangle \langle 0 | \bar{s} \gamma_\mu \gamma_5 d | K^0 \rangle} \quad (1.1)$$

is one of the fundamental weak matrix elements which have to be determined theoretically for deducing CP violation phase of the Cabibbo-Kobayashi-Maskawa matrix from experiments. Lattice QCD calculation may be an ideal tool to determine the matrix element precisely from the first principle. An essential step towards precise determination of B_K is to control systematic error in the renormalization factor. Recently non-perturbative renormalization factor is preferably employed to remove errors in the perturbative one. Among several non-perturbative schemes on the lattice the Schrödinger functional (SF) scheme [1] has an advantage that systematic errors can be evaluated in a controlled manner.

A few years ago the CP-PACS collaboration calculated B_K using quenched domain-wall QCD (DWQCD) with Iwasaki gauge action [8]. Their result was renormalized perturbatively at one loop and have shown a good scaling behavior with small statistical errors. A main purpose of this paper is to derive a non-perturbative renormalization factor \mathcal{Z}_{B_K} which convert the bare B_K of the CP-PACS collaboration to the renormalization group invariant (RGI) \hat{B}_K . We adopt the SF scheme as an intermediate scheme to avoid systematic uncertainties due to the finite lattice spacing. The renormalization factor $\mathcal{Z}_{B_K}(g_0)$ is given at a fixed bare coupling and its non-perturbative evaluation is decomposed into three steps in the SF scheme as

$$\mathcal{Z}_{B_K}(g_0) = Z_{VA+AV}^{\text{PT}}(\infty, \mu_{\text{max}}) Z_{VA+AV}^{\text{NP}}(\mu_{\text{max}}, \mu_{\text{min}}) Z_{B_K}^{\text{NP}}(g_0, \mu_{\text{min}}). \quad (1.2)$$

We start from a renormalization factor at a low energy hadronic scale μ_{min}

$$Z_{B_K}^{\text{NP}}(g_0, \mu_{\text{min}}) = \frac{Z_{VV+AA}(g_0, \mu_{\text{min}})}{Z_A^2(g_0)}, \quad (1.3)$$

where Z_{VV+AA} is a renormalization factor for the parity even part of the left-left four-quark operator and Z_A is that for the axial vector current. A reason why we define the renormalization factor at the hadronic scale is to suppress lattice artifacts by a condition $a\mu_{\text{min}} \ll 1$. This factor depends on both renormalization scheme and lattice regularization. Multiplying it with a lattice bare operator, the regularization dependence is canceled and only the scheme dependence remains.

$Z_{VA+AV}^{\text{NP}}(\mu_{\text{max}}, \mu_{\text{min}})$ represents non-perturbative RG running of the parity odd part of the left-left four-quark operators from the low energy scale μ_{min} to a high energy scale $\mu_{\text{max}} = 2^7 \mu_{\text{min}}$, where perturbation theory can be safely applied. Among three steps this requires the most extensive calculation. Since this factor evaluated in the continuum limit does not depend on a specific lattice regularization, we can employ $Z_{VA+AV}^{\text{NP}}(\mu_{\text{max}}, \mu_{\text{min}})$ evaluated previously by the Alpha collaboration with the improved Wilson fermion action[2], instead of calculating it by ourselves. Even though renormalization factors for the parity even and parity odd parts differ on the lattice without chiral symmetry, the difference disappears in the continuum limit, where the chiral symmetry is recovered.

The last factor $Z_{VA+AV}^{\text{PT}}(\infty, \mu_{\text{max}})$ is the RG evolution from the high energy scale μ_{max} to infinity, which absorb the scale dependence to give the RGI operator. Since we are already deep in a perturbative region at μ_{max} we can evaluate this factor perturbatively. Two loop calculation is given in Ref. [3]. Note that scheme dependence is also canceled at this stage and the RGI operator becomes scheme independent.

Our target in this study is the calculation of the first factor $Z_{B_K}^{\text{NP}}(g_0, \mu_{\text{min}})$. In order to further reduce the computational cost we use a relation that $Z_V = Z_A$ implied by the chiral symmetry of DWQCD in SF scheme [4], together with another one that $Z_{VV+AA} = Z_{VA+AV}$, which will be numerically checked later, and adopt the following definition throughout this paper,

$$Z_{B_K}(g_0, \mu) = \frac{Z_{VA+AV}(g_0, \mu)}{Z_V^2(g_0)}. \quad (1.4)$$

2. Renormalization conditions for four-quark operator

Since we utilize the step scaling function (SSF) obtained by the Alpha collaboration [2] as an intermediate RG running factor from μ_{min} to μ_{max} , the same renormalization scheme should be adopted for our calculation of $Z_{B_K}^{\text{NP}}(g_0, \mu_{\text{min}})$. The renormalization condition is given by the following correlation function [2]

$$\mathcal{F}_{\Gamma_A \Gamma_B \Gamma_C}(x_0) = \frac{1}{L^3} \langle \mathcal{O}_{21}[\Gamma_A] \mathcal{O}_{45}[\Gamma_B] \mathcal{O}_{VA+AV}(x) \mathcal{O}'_{53}[\Gamma_C] \rangle, \quad (2.1)$$

where subscripts 1 ~ 5 represent quark flavours and \mathcal{O}_{VA+AV} is the parity odd four quark operator which consists of four different flavours from 1 to 4. Boundary operators \mathcal{O}_{ij} and \mathcal{O}'_{ij} are given in terms of boundary fields ζ and ζ' [1] as

$$\mathcal{O}_{ij}[\Gamma] = a^6 \sum_{\vec{x}\vec{y}} \bar{\zeta}_i(\vec{x}) \Gamma \zeta_j(\vec{y}), \quad \mathcal{O}'_{ij}[\Gamma] = a^6 \sum_{\vec{x}\vec{y}} \bar{\zeta}'_i(\vec{x}) \Gamma \zeta'_j(\vec{y}). \quad (2.2)$$

Due to the SF boundary condition for fermion fields the boundary operator should be parity odd and we have two independent choices $\Gamma = \gamma_5$ and $\Gamma = \gamma_k$ ($k = 1, 2, 3$). For the correlation function to be totally parity-even we need at least three boundary operators in (2.1). Logarithmic divergences in boundary fields ζ 's can be removed by the boundary-boundary correlation functions;

$$f_1 = -\frac{1}{2L^6} \langle \mathcal{O}'_{12}[\gamma_5] \mathcal{O}_{21}[\gamma_5] \rangle, \quad k_1 = -\frac{1}{6L^6} \sum_{k=1}^3 \langle \mathcal{O}'_{12}[\gamma_k] \mathcal{O}_{21}[\gamma_k] \rangle. \quad (2.3)$$

We adopt the following three choices [2], whose perturbative expansions behave reasonably well [3]:

$$h_1^\pm(x_0) = \frac{\mathcal{F}_{[\gamma_5, \gamma_5, \gamma_5]}(x_0)}{f_1^{3/2}}, \quad h_3^\pm(x_0) = \frac{\frac{1}{3} \sum_{k=1}^3 \mathcal{F}_{[\gamma_5, \gamma_k, \gamma_k]}(x_0)}{f_1^{3/2}}, \quad h_7^\pm(x_0) = \frac{\frac{1}{3} \sum_{k=1}^3 \mathcal{F}_{[\gamma_5, \gamma_k, \gamma_k]}(x_0)}{f_1^{1/2} k_1}. \quad (2.4)$$

We call three renormalization schemes defined through these correlation functions as scheme 1, 3, 7 according to the Alpha collaboration [2].

We impose the following renormalization condition

$$Z_{VA+AV;s}^\pm(g_0, \mu) h_s^\pm(x_0 = L/2; g_0) = h_s^{\pm(\text{tree})}(x_0 = L/2) \quad (2.5)$$

N_L	6	8	10	12	14	16	18
β	2.4446	2.6339	2.7873	2.9175	3.0313	3.1331	3.2254
$\mathcal{Z}_{B_K;1}(g_0)$	1.22(2)	1.32(2)	1.35(2)	1.39(2)	1.40(2)	1.41(3)	1.42(3)

Table 1: β values which gives the same box size $2L_{\max}$ for each lattice sizes N_L .

where s labels the scheme. This means that the renormalized correlation function should coincides with that at tree level in the continuum at the middle of the box $x_0 = L/2$. The renormalization scale at the low energy (hadronic scale) is introduced by the maximum box size $1/\mu_{\min} = 2L_{\max}$, where L_{\max} is defined through renormalized coupling $\bar{g}^2(1/L_{\max}) = 3.480$ in the SF scheme. This box size corresponds to $L_{\max}/r_0 = 0.749(18)$ [5] in the continuum limit, so that $\mu_{\min} = 1/2L_{\max} \sim 263$ MeV using the Sommer scale $r_0 = 0.5$ fm.

3. Numerical simulation details

The CP-PACS collaboration has calculated the lattice bare B_K in quenched DWQCD with Iwasaki gauge action at the domain wall height $M = 1.8$ and the fifth dimensional length $N_5 = 16$ [8]. In order to renormalize this B_K we adopted the same lattice formulation as in the above. The SF formalism for Iwasaki gauge action is given in Ref. [5]. For a domain-wall quark we adopted the orbifolding construction [6] to realize the SF boundary condition. We employ the same size for the temporal and the spatial directions $T = L$. We take the mass independent scheme in massless limit where all the physical quark masses are set to zero.

Three lattice spacings $\beta = 2.6, 2.9$ and 3.2^1 are employed corresponding to $a^{-1} \sim 2, 3$ and 4 GeV in the previous simulation [8]. In order to cover these three β 's we take 7 lattice sizes. At each lattice size we tune β to satisfy $aN_L = 2L_{\max} = 1.498r_0$ using the following fit formula [5]

$$\ln\left(\frac{a}{r_0}\right) = -2.193 - 1.344(\beta - 3) + 0.191(\beta - 3)^2, \quad (3.1)$$

which covers $2.456 \leq \beta \leq 3.53$. Lattice sizes and corresponding β values are listed in Table 1.

Quenched gauge configurations are generated by using the HMC algorithm. First 2000 trajectories were discarded for thermalization. We calculate the correlation functions on each configuration separated by 200 trajectories. We employed 500 to 1000 configurations in this paper.

4. Non-perturbative renormalization of B_K

In this section we evaluate the renormalization factor $\mathcal{Z}_{B_K;s}(g_0)$, which convert the lattice bare $B_K(g_0)$ in DWQCD to the RGI \hat{B}_K . Combining our renormalization factor $Z_{B_K;s}^{\text{NP}}(g_0, \mu_{\min})$ with the RG running factor $Z_{VA+AV}^{\text{PT}}(\infty, \mu_{\max})Z_{VA+AV}^{\text{NP}}(\mu_{\max}, \mu_{\min})$ given by the Alpha collaboration, we obtain the renormalization factor $\mathcal{Z}_{B_K;s}(g_0)$ at each β . A result is given in Table 1 for scheme 1. In order to obtain the renormalization factors at $\beta = 2.6, 2.9$ and 3.2 we fit it in a polynomial form, $\mathcal{Z}_{B_K;s}(g_0) = a_s + b_s(\beta - 3) + c_s(\beta - 3)^2$.

¹The data at $\beta = 3.2$ is new and not published in [8]

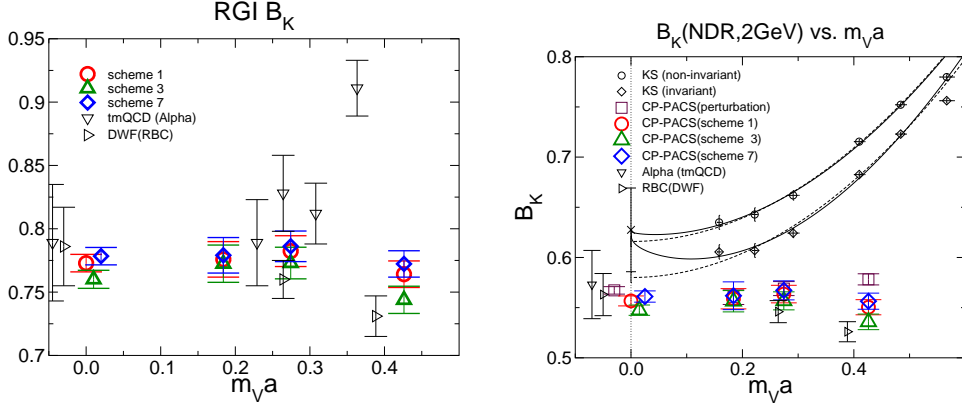


Figure 1: Scaling behavior of RGI \hat{B}_K (left panel) and $B_K(\overline{\text{MS}}, 2\text{GeV})$ (right panel). Our results are shown by open circle (scheme 1), open up triangle (scheme 3) and open diamond (scheme 7). Previous results with tmQCD [2] and DWF [9] are also shown by open down and right triangles. In the right panel result of the KS fermion [7] and DWF [8] with perturbative renormalizations are also given. The continuum results are slightly shifted to avoid overlaps.

Multiplying it to the bare $B_K(g_0)$ we obtain the RGI \hat{B}_K , whose scaling behavior is shown in the left panel of Fig. 1. We also evaluate the renormalized B_K in $\overline{\text{MS}}$ scheme with naive dimensional regularization (NDR) at a scale $\mu = 2\text{ GeV}$. The scaling behavior of $B_K^{\overline{\text{MS}}}(\text{NDR}, 2\text{GeV})$ is given in the right panel of Fig. 1. Since the scaling violation is negligible, it is reasonable to take the continuum limit by a constant extrapolation. We arrival at $\hat{B}_K = 0.773(7)_{(-13}^{+5})$ and $B_K^{\overline{\text{MS}}}(\text{NDR}, 2\text{GeV}) = 0.557(5)_{(-10}^{+4})$, where central values are taken from the scheme 1, the first parenthesis gives statistical error, and upper(lower) error in the second parenthesis denotes difference between schemes 1 and 7(1 and 3). These are main results in this study.

5. Additional investigations

We perform two additional calculations. One is to study the scaling behavior of SSF defined by $\Sigma_{VA+AV;s}^{\pm}(u, a/L) = \frac{Z_{VA+AV;s}^{\pm}(g_0, a/2L)}{Z_{VA+AV;s}^{\pm}(g_0, a/L)} \Big|_{g^2(1/L)=u}$ in DWQCD. The other is to investigate a size of chiral symmetry breaking effects in renormalization factors.

5.1 Scaling behavior of SSF at $u = 3.480$

We investigate the SSF at strong coupling, $u = \bar{g}^2(1/L_{\text{max}}) = 3.480$, for four different β 's. In the left panel of Fig. 2 we show a dependence of our SSF (open square) and the continuum limit of the Alpha collaboration [2] (star). We find that scaling violation of our SSF is large and oscillating at $M = 1.8$. We speculate that this bad scaling behavior is caused by the $\mathcal{O}(a)$ boundary effect in the SF scheme of DWQCD, not by the $\mathcal{O}(a)$ bulk chiral symmetry breaking effect. To see this we calculate the SSF at tree level, where $N_5 \rightarrow \infty$ limit is already taken. We plot its scaling behavior by open circles in the left panel of Fig 3, where the similar sort of oscillating behavior is observed at $M = 1.8$. To exclude a possibility that the large scaling violation is caused by the bulk chiral symmetry breaking effect, we calculate N_5 dependence directly at $u = 3.480$. Indeed comparisons

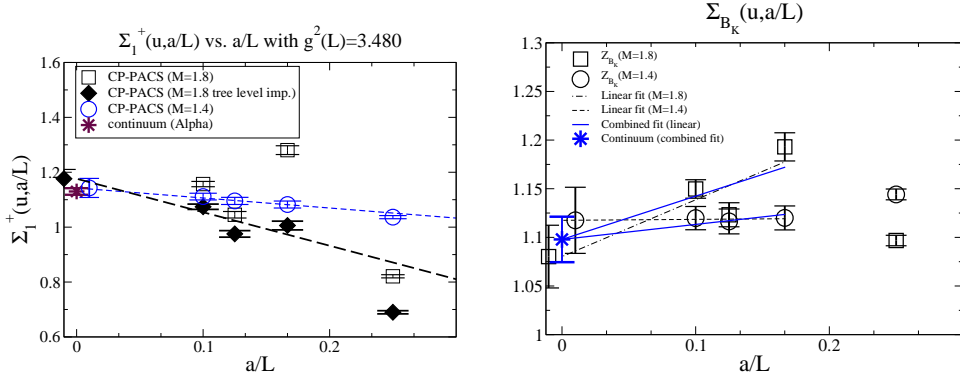


Figure 2: Scaling behavior of SSF for $Z_{VA+AV;1}$ (left panel) and for Z_{B_K} (right panel). Open squares are results for $M = 1.8$ and open circles are for $M = 1.4$ without improvement. Filled diamonds denote results for $M = 1.8$ with tree level improvement. Star symbol denotes the continuum limit.

between $N_5 = 8$ and $N_5 = 16$ for $\Sigma_{VA+AV;s}(u, L/a = 4)$ and between $N_5 = 32$ and $N_5 = 16$ for $\Sigma_{VA+AV;s}(u, L/a = 6)$ show no N_5 dependence within statistical errors.

We find that the scaling behavior of the tree SSF is much improved at $M = 0.9$, as shown in the left panel of Fig 3. This suggests that the scaling behavior of the non-perturbative SSF is also improved when the renormalized domain-wall height is nearly equal to unity. We first evaluate the SSF at $M = 1.4$, where tadpole improved domain-wall height is nearly equal to unity. Result is given by open circles in the left panel of Fig 2. We find good scaling behavior at $M = 1.4$, and the linear continuum extrapolation is consistent with the continuum limit of the Alpha collaboration.

For another improvement we introduce a tree level improvement, where the continuum tree level correlation function $h_s^{\pm(\text{tree})}(x_0)$ in the renormalization condition (2.5) is replaced to that on the lattice $h_s^{\pm(\text{tree})}(x_0)^{\text{LAT}}$. We expect that the large scaling violation of the SSF is partly canceled by the tree SSF. We calculate the tree level improved SSF, where the tadpole improved value $M \sim 1.5$ of $M = 1.8$ at each β is used for $h_s^{\pm(\text{tree})}(x_0)$. The result is given by the filled diamond in the left panel of Fig 2. We find that the scaling behavior is improved, so that we can perform a linear extrapolation to the continuum limit, whose value is consistent with that of the Alpha collaboration.

Furthermore we calculate the SSF of B_K , defined by $\Sigma_{B_K}(u, a/L) = \frac{Z_{B_K}(g_0, a/2L)}{Z_{B_K}(g_0, a/L)}$. The result is plotted in the right panel of Fig 2 by open square ($M = 1.8$) and open circle ($M = 1.4$). We find that a large scale violation in Σ_1^+ is partly canceled in Σ_{B_K} at $M = 1.8$. Linear continuum extrapolations using data at finest three lattice spacings give consistent values between $M = 1.4$ and $M = 1.8$.

5.2 Chiral symmetry breaking effect

We check whether the chiral relation that $Z_{VV+AA} = Z_{VA+AV}$ we assumed is realized or not in our DWQCD. If the chiral symmetry were exact we would have a chiral WT identity

$$\langle O_{VA+AV} \mathcal{O}[\zeta] \rangle_S = \langle O_{VV+AA} \tilde{\mathcal{O}}[\zeta] \rangle_S \quad (5.1)$$

under chiral rotation of the first flavour $\delta q_1 = -i\gamma_5 \tilde{q}$, $\delta \zeta_1 = i\gamma_5 \tilde{\zeta}_1$, $\delta \zeta'_1 = i\gamma_5 \tilde{\zeta}'_1$, where $\tilde{\mathcal{O}}[\zeta]$ is a chiral rotation of some boundary operator (2.2). We get a relation $Z_{VV+AA} = Z_{VA+AV}$ from this WT identity. On the other hand, the domain-wall fermion action is not invariant under the chiral

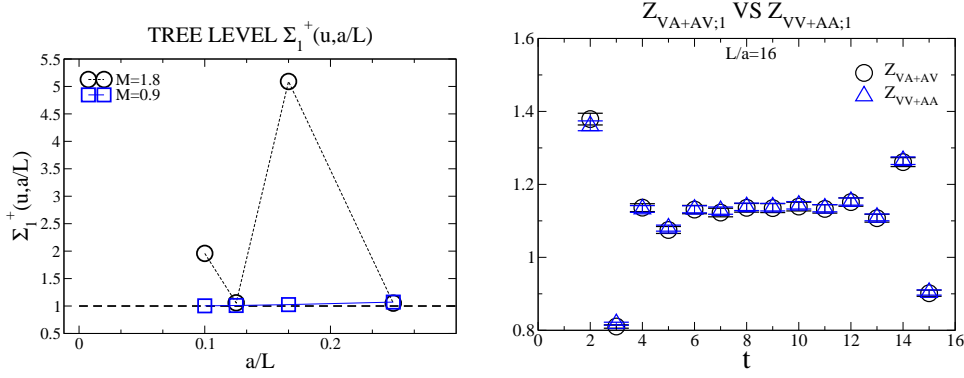


Figure 3: Left panel is a scaling behavior of tree level SSF. Open circle shows results with $M = 1.8$ and open square shows those with $M = 0.9$. Right panel is a comparison between $Z_{VA+AV}(g_0, \mu_{\min})$ (open circle) and $Z_{VV+AA;1}(g_0, \mu_{\min})$ (open triangle) as a function of time t . We adopt scheme 1 at the hadronic scale μ_{\min} on $L/a = 16$ lattice.

rotation as $S_{\text{dwf}} \rightarrow S_{\text{dwf}} + Y$, where $Y = \bar{\psi}X\psi$ is the chiral symmetry breaking term at the middle of the fifth dimension. Therefore the WT identity becomes $\langle O_{VA+AV} \mathcal{O}[\zeta] \rangle_S = \langle O_{VV+AA} \tilde{\mathcal{O}}[\zeta] \rangle_{S+Y} \neq \langle O_{VV+AA} \tilde{\mathcal{O}}[\zeta] \rangle_S$, and we estimate a possible chiral symmetry breaking effect by directly comparing $\langle O_{VA+AV} \mathcal{O}[\zeta] \rangle_S$ with $\langle O_{VV+AA} \tilde{\mathcal{O}}[\zeta] \rangle_S$. We evaluate the renormalization factor $Z_{VV+AA}(g_0, \mu_{\min})$ using the chirally rotated correlation function with 100 configurations at each β . The right panel of Fig 3 shows a time dependence of Z_{VA+AV} and Z_{VV+AA} at $L/a = 16$. We observe a good agreement between them, and similar results are obtained at other L/a . Therefore the relation $Z_{VV+AA} = Z_{VA+AV}$ is realized in our simulations.

This work is supported in part by Grants-in-Aid for Scientific Research from the Ministry of Education, Culture, Sports, Science and Technology(Nos.18740130).

References

- [1] S. Sint, Nucl. Phys. Proc. Suppl. **94** (2001) 79 and references therein.
- [2] ALPHA Collaboration, M. Guagnelli *et al.*, JHEP **0603** (2006) 088.
- [3] F. Palombi, C. Pena and S. Sint, JHEP **0603** (2006) 089.
- [4] CP-PACS Collaboration, S. Aoki *et al.*, Phys. Rev. **D70** (2004) 034503.
- [5] CP-PACS Collaboration, S. Takeda *et al.*, Phys. Rev. **D70** (2004) 074510.
- [6] Y. Taniguchi, JHEP **0610** (2006) 027.
- [7] S. Aoki *et al.* [JLQCD Collaboration], Phys. Rev. Lett. **80** (1998) 5271.
- [8] A. Ali Khan *et al.* [CP-PACS Collaboration], Phys. Rev. D **64** (2001) 114506.
- [9] Y. Aoki *et al.*, Phys. Rev. D **73** (2006) 094507.